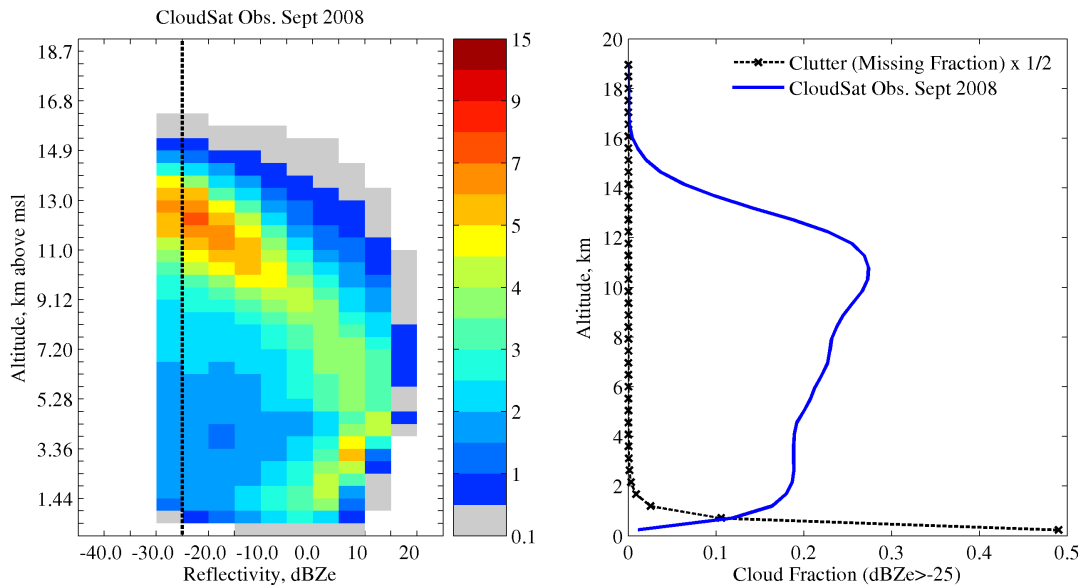


CloudSat Reflectivity-Height Histogram (cfadDbze94) Data Description and Quality Statement, March 2019

Roger Marchand (rojmarshand@u.washington.edu)

1. Overview

The CloudSat Reflectivity-Height Histogram product (also known by the CMIP variable name cfadDbze94) contains 2D histograms (joint distributions) of the CloudSat observed radar reflectivity factor (in dBZe) with altitude above mean sea level, as depicted in the left panel of Figure 1. The data are monthly and stored on a simple 2 x 2 degree fixed latitude by longitude grid, and using a vertical (altitude) grid with 480 m vertical spacing.



The data file contains information on the number of CloudSat columns (the number of radar profiles) and satellite overpasses associated with each 2 x 2 degree grid cell, such that histograms can be aggregated over any combination of grid cells, and sampling uncertainties estimated. Figure 1, for example, covers a large region in Tropical Western Pacific. Likewise, the data can easily be used to calculate vertical profiles of hydrometeor occurrence (relative to a given threshold for the reflectivity) by simply summing the fractional occurrence over any desired range of reflectivity bins. The right panel of Figure 1, for example, shows the mean profile of hydrometer occurrence for the Tropical Western Pacific, while Figure 2, shows the zonal mean profile of hydrometeor occurrence for hydrometeors with a reflectivity factor > -25 dBZe.

Figure 1 – Example of CloudSat Reflectivity Height histogram. Data shown is for the Tropical Western Pacific, Sept. 2008. The radar does not detect weakly reflecting hydrometeors well, which is one reason why it is important to account for the radar sensitivity in any comparison of the CloudSat observations with model output. The data here are restricted to measured reflectivity factors greater than -30 dBZe. The lack of detections below 1 km is due to surface clutter. The fraction of data lost in the clutter is shown by the dashed black line in the right panel, along with the mean profile of hydrometeor occurrence with a reflectivity > -25 dBZe.

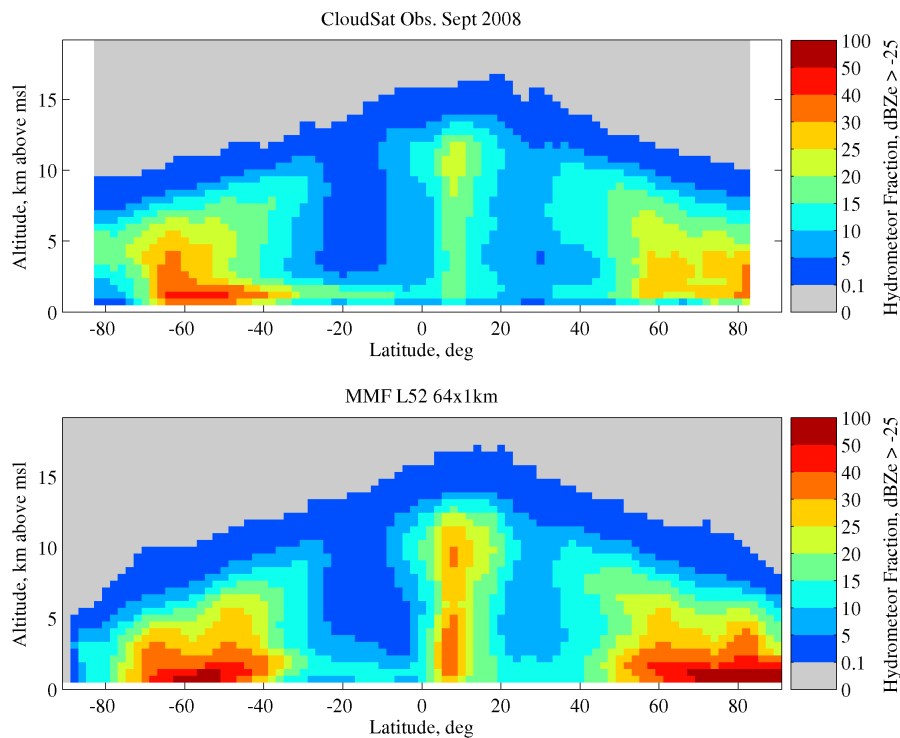


Figure 2 - Example of Zonal mean profile of hydrometeor occurrence for Sept. 2008 from (top) this dataset (bottom) simulated from the MMF model using COSP simulator (following Marchand et al. [2009]). Note the CloudSat observations are limited to latitudes between $\sim 82^\circ$ N/S.

Part of the intent for producing these data is that they be used in the evaluation of climate model output. When used for this purpose I strongly encourage model output be generated using the CFMIP Observation Simulator Package (COSP, Bodas-Salcedo et al. 2001, code available at <https://github.com/CFMIP/COSPv2.0>). Figure #2 show an example of COSP simulated data (form the MMF model).

I also strongly caution users to be aware of the changes in this CloudSat data resulting from the implementation of Daylight Only Operations (DOOP) in May 2012, which is detailed in the next section, and to tailor their use of these data appropriately. I welcome users who are unclear on DOOP or who want to discuss the situation to contact me via the email address given at the top of this document.

Section 3 describes the key variables included in the data set, Section 4 describes the processing, and Section 5 discusses limitations of the data (other than DOOP).

2. Orbital Characteristics & Daylight Only Operations

On April 17th, 2011, a battery anomaly caused CloudSat to stop collecting data and lose formation with the A-Train. The radar was eventually turned back on in November 2011, but it was not until May 15, 2012, that the satellite returned to (near) its original position in the A-Train. Since the battery anomaly, the radar is only able to operate while the sun

is actively shining on the satellite solar panels. In fact, the satellite goes through a complex set of maneuvers on each orbit where the radar is turned off and the satellite is spun to stabilize it as it enters the Earth's shadow, after which the spin is halted and the radar restarted once the satellite leaves the Earth's shadow. The exact nature of this mode of operations has changed slightly over time, and is collectively referred to as Daylight Only Operations (or DOOP). DOOP has significant implication for the mission, resulting in a dramatic change in the radar sampling and necessitates some discussion of the CloudSat orbital characteristics.

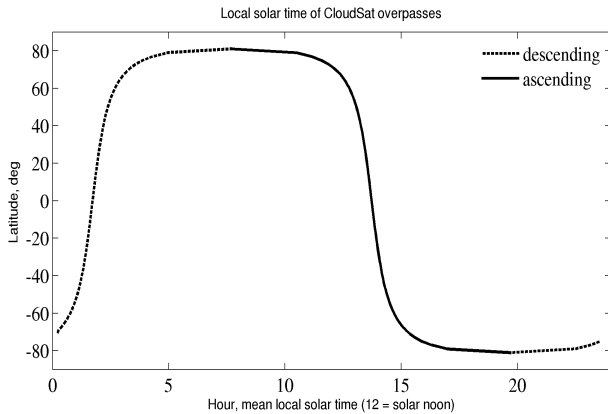


Figure 3 - CloudSat mean local solar overpass time (Sept. 2006).

CloudSat is in a sun-synchronous orbit meaning that each time the satellite passes over any given point on the Earth it does so at (nearly) the same local mean solar time on each overpass, and this time depends on the latitude. Figure 3 shows the mean local solar time of CloudSat overpasses, where local solar noon is 12 hours. Here the dashed line is when the satellite is descending (going from north to south) and the solid line is when the satellite is ascending (going from south to north). The equator crossing time is at about 1:45 pm mean local solar time on the ascending node and 1:45 am on the descending node. The equator crossing time (for all the data included in this dataset) varies by less than about 5 minutes. Data collected between +/- 40° N is collected within 30 minutes of the equator crossing time and +/- 60° N is collected within 1 hour of the equator crossing time (on each node), while at higher latitudes data are collected over a much wider time window.

The present Reflectivity-Height dataset includes the following six variables, which give the mean, minimum and maximum of the (local solar) sampling time associated with each 2° latitude bin for the ascending and descending node, respectively, in each month.

mean_local_sampling_time_ascending (time, lat_bin)
min_local_sampling_time_ascending (time, lat_bin)
max_local_sampling_time_ascending (time, lat_bin)
mean_local_sampling_time_descending (time, lat_bin)
min_local_sampling_time_descending (time, lat_bin)
max_local_sampling_time_descending (time, lat_bin)

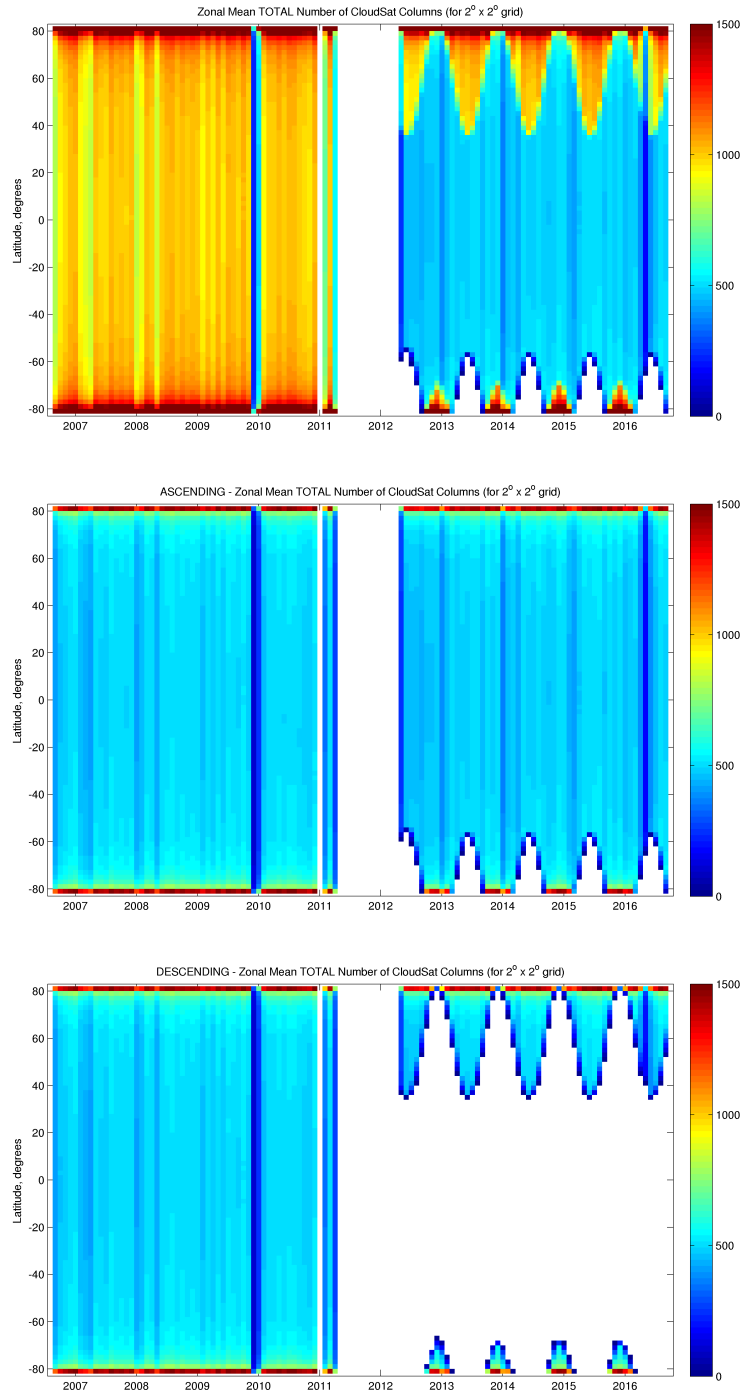


Figure 4 - Zonal mean of the number of CloudSat columns that contribute to each 2 x 2 degree grid cell (top) total = ascending + descending, (middle) ascending only, (bottom) descending only

Prior to the battery anomaly, sampling was equal on the ascending and descending nodes. Figure 4 depicts the zonally average number of CloudSat columns, which contribute data to each 2 x 2 degree latitude by longitude grid cell for each month of the mission between Sept 2006 and Sept. 2016. The large white gap in the middle of the figure panels is the period where CloudSat was out of the A-train. (CloudSat was not transmitting for much of this time, but there is also some data that we have excluded from this Reflectivity-Height Histogram summary product due to several complexities).

As the top panel in Figure 4 shows, the sampling during DOOP (after May 2012) has a strong seasonal component. Only at high latitudes in the Northern Hemisphere (NH) summer and a very small region in the SH summer is the total sampling the same as pre-DOOP. Also, a significant portion of the SH high latitudes (extending to almost 55° S at its maximum) is entirely unsampled during the SH winter. The middle and lower panels show how the changes are related to the ascending and descending nodes. This is all due to the loss of data when the satellite is in the Earth's shadow (or otherwise preparing to enter or leave the shadow).

For all of the key variables included in the file (including the primary variables *cfadDbze95* – see section 3) **there are “_ascending” and “_descending” versions of the variables**, which restrict the data to the ascending or descending node.

In addition, the data includes two flag variables.

is_sampled_during_DOOP_ascending (time, lat_bin)
is_sampled_during_DOOP_descending (time, lat_bin)

The value of this flag is true (value = 1) if a given latitude bin is sampled during DOOP (since May 2012) at a rate > 80% of that which occurred before DOOP.

3. Key variables

cfadDbze94 (time, dbze bin, height bin, lat bin, lon bin),

The primary variable contained in the file is a histogram called *cfadDbze94*. The variable has 5 dimensions (time, reflectivity bin, height bin, latitude bin, longitude bin) with one entry per month. The histogram contains frequency-of-occurrence information. That is, how often does CloudSat detect a hydrometeor within a given altitude range (defined by the variables *alt40* and *alt40_bnds*) and with a given range of reflectivity factors (specified by variables *dbze* and *dbze_bnds*).

NOTE variables *cfadDbze94_ascending(...)* and *cfadDbze94_descending(...)* are the same but restricted to data collected during the ascending or descending nodes, respectively.

columns (time, lat bin, lon bin),

The total number of radar columns or profiles contributing data in each latitude and longitude bin, in each month.

overpasses (time, lat bin, lon bin),

The total number of orbits contributing data to each latitude and longitude bin, in each month. Note: data from nearby-in-time-and-space radar columns/profiles are highly correlated. For purposes of determining uncertainty bounds due to sampling, I recommend treating each overpass as an independent sample.

missingdatafraction (time, latitude bin, longitude bin)

The fraction of CloudSat resolution volumes that contain clutter at each altitude, and in each latitude and longitude bin in each month. See discussion of surface clutter in section 5.

4. Brief Description of Processing:

The reflectivity-height histogram data is based on the hydrometeor-mask and reflectivity measurements contained in the operational CloudSat 2B-GeoProf data product (Marchand et al. 2008). We note that the hydrometeor-mask is often called a “cloud mask” even though the radar reflectivity is due to both clouds and precipitation (collectively hydrometeors). The presented dataset was produced in January 2018, from GeoProf release/version P1rc_R05 (see also data file global attribute `source_version_number`) and covers the period Sept. 2006 through Sept. 2016.

The histograms (*cfadDbze94*) contain frequency-of-occurrence information, and are constructed by counting how often CloudSat detected a hydrometeor with a confidence (mask) value of 20 AND a reflectivity value greater than or equal to -30 dBZe. These thresholds ensure a low false detection rate (Marchand et al. 2008). CloudSat radar range-resolution-volumes that do not meet both of these thresholds are considered clear-of-hydrometeors. That is, each CloudSat radar-resolution volume is given a value of 1 or 0 based on the above thresholds.

The histogram frequency of occurrence is then determined by assigning each radar resolution volume to a specific histogram height bin based on the midpoint altitude of the radar-resolution volume AND a specific histogram dbze bin based on the measured reflectivity factor. The frequency of occurrence in each histogram height x dbze bin is then calculated as the sum of hydrometeor occurrences (sum of values = 1) for the given height bin and dbze bin divided by the total number of possible occurrences (sum of values = 1 or zero) for the given height bin.

Thus, summing the frequency of occurrences across dBZe bins will yield a value between 0 and 100%, BUT summing down height bins (for a fixed value of dBZe) will yield a value greater than 100% (because the radar signal penetrates most clouds and precipitation and can contribute counts at multiple altitudes). The histogram height bins are 480 m wide, such that (on average) each histogram height bin will have 2 CloudSat reflectivity measurements on average. But because the CloudSat altitudes vary from column to column, any given radar column may contribute 1, 2 or 3 samples to the histogram height bin.

Range-resolution-volumes with a hydrometeor-mask-value of 5 AND a reflectivity value greater than or equal to -25 dBZe in the CloudSat data are indicative of surface clutter and the variable *missingdatafraction* is used to track how often this occurs using the same approach as described above for *cfadDbze94* (except that all the counts are placed into a single reflectivity bin, meaning I do not provide the frequency as a function of clutter reflectivity, only the mean frequency of occurrence of clutter with altitude).

4. Known Problems/Limitations:

(1) Surface Clutter

Perhaps the most significant limitation of the CloudSat observations (and this dataset) is reduced sensitivity near the surface due to ground clutter; that is echo power coming from the surface adds to the total observed reflectivity making it difficult to discern whether or not hydrometeors are present. For CloudSat, this region of surface clutter extends to approximately 1 km above the surface. At 500 m above the surface, only strong precipitation can be unambiguously identified. See Marchand et al. [2008] for additional information.

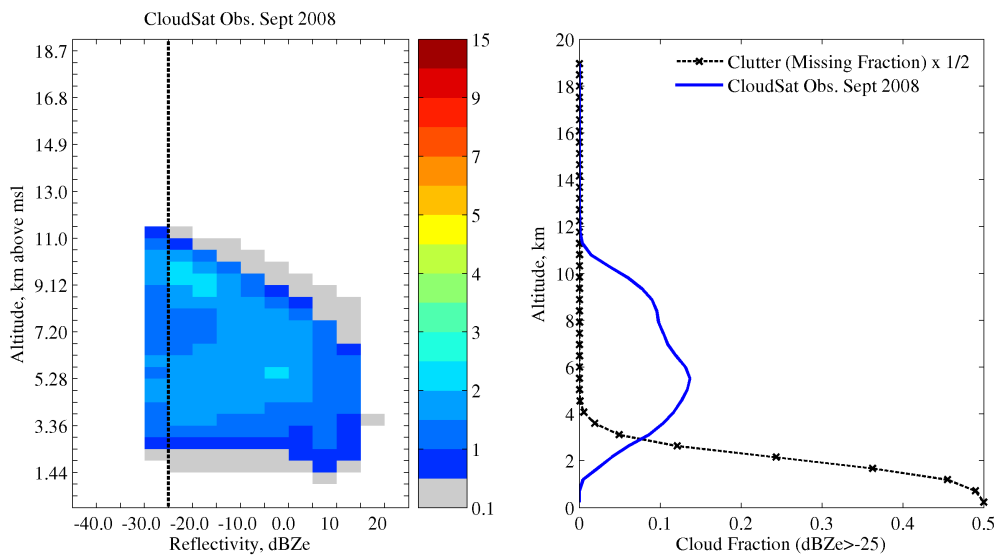


Figure 5 - Same as Figure 1 but for the Western United States, including most of the Rocky Mountains. Note the missing-data fraction plotted has been multiplied by 0.5 to make the values easier to read.

The variable *missingdatafraction* (see section 3) indicates the amount of data missing due to clutter as a function of the height bin (that is, the distance above mean sea level). Over 2° degree grid cells that contain only ocean the impact is only serious for the first two height bins (see for example Figure #1). Over land, variations in the topography and clutter limit sampling, as shown in Figure #5 for data aggregated over the U.S. Rockies.

(2) Sensitivity

At the start of the mission, CloudSat had a sensitivity (that is a minimum detectable signal) of somewhat better than -30 dBZe. This has dropped over the course of the mission, but is expected to remain above -25 dBZe (for at least the next few years).

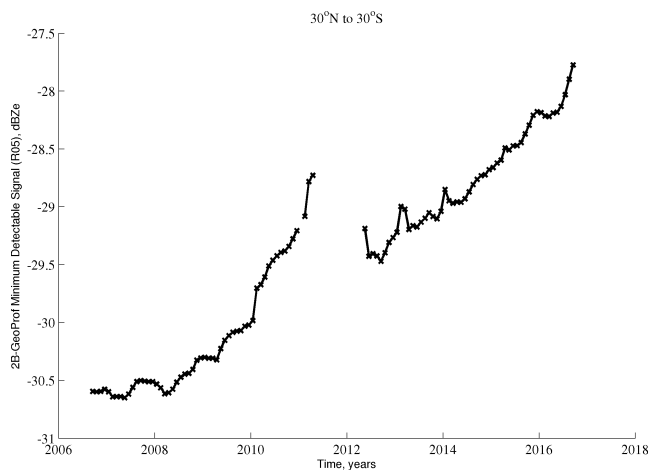


Figure 6 - Change in CloudSat Sensitivity between Sept. 2006 and Sept. 2016.

In this data set, I have removed data below the -30 dBZe (see section 3), such that reflectivity factors below -30 dBZe count as clear sky. That said, it should be noted that there is a statistically significant decrease in detections rates for reflectivity factors between -30 to -25 dBZe and a very slight decrease in detection rates between -25 and -20 dBZe over the duration of the mission. This is due to a reduction in the number of reflectivity measurements which pass the level 20 confidence threshold, as the sensitivity decreases. As such, in addition to accounting for DOOP sampling difference, these data should be used cautiously for any trend analysis (or comparison of data from the early and late mission) for these relatively low reflectivity factors.

A “**constant sensitivity**” version of the GeoProf data is currently being designed. This data product will have less sensitivity than the current operational CloudSat products – essentially reducing the sensitivity of all measurements to a constant level - but will be more suitable for trend analysis. Users interested in these data are encouraged to contact me directly (using the email address given at the top of this document).

5. References

Bodas-Salcedo, A., M.J. Webb, S. Bony, H. Chepfer, J. Dufresne, S.A. Klein, Y. Zhang, R. Marchand, J.M. Haynes, R. Pincus, and V.O. John, 2011: COSP: Satellite simulation

software for model assessment. *Bull. Amer. Meteor. Soc.*, 92, 1023–1043, doi:10.1175/2011BAMS2856.1

Marchand, R., J. Haynes, G. G. Mace, T. Ackerman, and G. Stephens (2009), A comparison of simulated cloud radar output from the multiscale modeling framework global climate model with CloudSat cloud radar observations, *J. Geophys. Res.*, 114, D00A20, doi:10.1029/2008JD009790.

Marchand, R., G.G. Mace, T. Ackerman, and G. Stephens (2008), Hydrometeor Detection Using Cloudsat—An Earth-Orbiting 94-GHz Cloud Radar. *J. Atmos. Oceanic Technol.*, 25, 519–533.

Zhang, Y., S. A. Klein, J. Boyle, and G. G. Mace (2010), Evaluation of tropical cloud and precipitation statistics of Community Atmosphere Model version 3 using CloudSat and CALIPSO data, *J. Geophys. Res.*, 115, D12205, doi:10.1029/2009JD012006.